Transition Metal Chemistry
https://doi.org/10.1007/s11243-019-00362-y

Ruthenium [NNN] and [NCN]-type pincer complexes with phosphine coligands: synthesis, structures and catalytic applications

Bo Zhang[1] · Haiying Wang[1] · Xuechao Yan[1] · Yu-Ai Duan[1] · Shuai Guo[1] · Fei-Xian Luo[2]

Received: 4 September 2019 / Accepted: 25 October 2019

Abstract

A series of ruthenium [NNN]- or [NCN]-type complexes (**3**–**7**) bearing PPh_3 ancillary ligands have been synthesized from pyridine- or phenylene-bridged bis(triazoles) **1** and **2**. In the case of [NNN]-pincer complex **3**, an unusual and unexpected *cis*-orientation adopted by two sterically demanding PPh_3 ligands was observed, and such configuration proved to be unchanged in solution for a long time. By contrast and as expected, the two phosphines are found to be *trans* to each other in the case of [NCN]-type pincer complex **4**, but an oxidation of Ru^{II} center to Ru^{III} occurred. Complex *cis*-**3** underwent ligand exchanges leading to the formations of diphosphine derivatives **5** and **6**. As a representative, *cis*-**3** was treated with the base in isopropanol affording a mixture of Ru–hydrido complexes with various phosphine binding modes, one of which (*trans*-**7**) bearing two *trans*-standing phosphines has been successfully isolated and fully characterized. The catalytic performances of all newly synthesized Ru complexes have been examined and compared in transfer hydrogenations of ketones and enones, in which mono-phosphine complexes proved to be significantly superior to their diphosphine counterparts. The catalytic process proved to involve Ru–H key intermediates, but the *trans*-oriented Ru–H species is unlikely to be the main catalytic contributor. In particular, the best performer *cis*-**3** exhibits high chemoselectivity in certain cases catalyzing α,β-unsaturated ketones, whose behavior is quite different compared to most precedents.

Introduction

Pyridine-bridged [NNN]-pincer frameworks, as exemplified by *Pybox* and *Terpy*, have become "popular" ligands in transition metal chemistry and homogenous catalysis. In this regard, bis(1,2,3-triazol-4-yl)pyridines (btp, Fig. 1) have received increasing interest in recent years.[1] One appealing synthetic advantage of such type of ligands is that they can be very expediently constructed through simple Cu-catalyzed azide–alkyne cycloadditions (CuAACs),[2] making such motifs easily accessible and stereoelectronically tunable. Various btp-containing complexes have been documented, and this area has been comprehensively reviewed by Byrne and Gunnlaugsson et al. [1].

In respect of the coordination chemistry of btp ligands, ruthenium is undoubtedly the most extensively studied metal center. This is mainly owing to the promising optical property of Ru–btp complexes, and such complexes can be regarded as the homologues of the very successful Ru–Terpy complexes.[3] However, surprisingly and to the best of our knowledge, there is no catalytic investigation of Ru–btp complexes thus far, although Ru complexes supported by other types of [NNN]-pincer platforms have shown highly remarkable performance in many catalytic transformations[4] especially in THs (THs = transfer hydrogenations).[5,6] Thus, as a contribution to this less studied area, herein we report a series of Ru–phosphine pincer complexes **I** (Fig. 1) and their diphosphine derivatives, and systematically reveal their

Electronic supplementary material The online version of this article (https://doi.org/10.1007/s11243-019-00362-y) contains supplementary material, which is available to authorized users.

✉ Shuai Guo
guoshuai@cnu.edu.cn

[1] Department of Chemistry, Capital Normal University, Beijing, People's Republic of China

[2] College of Life and Environment Science, Minzu University of China, Beijing, People's Republic of China

[1] For a related review, see [1].

[2] For selected reviews, see [2–6].

[3] For recent papers focusing on the Ru–btp complexes and their photoluminescence applications, see [7–9].

[4] For selected reviews on Ru pincer complexes, see [10–13].

[5] For selected examples, see [14–20].

[6] For selected examples, see [20–27].

Published online: 14 November 2019

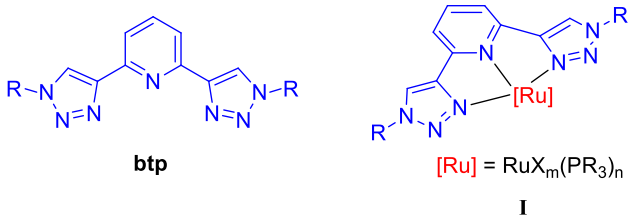

Fig. 1 Ligand btp and the target system (**I**) in this work

versatile phosphine binding behaviors, reactivities/stabilities, catalytic performances and mechanistic considerations in THs of ketones as well as enones.

Results and discussion

Synthesis of (pro)ligands

Pyridine- and phenylene-bridged bis(triazoles) **1** and **2**, which have been reported elsewhere [28–30], were synthesized via copper-catalyzed "click" reactions of benzyl azide (**A**) with commercially available alkynes **B** and **C**, respectively (Scheme 1). In an earlier study from our group [31], copper(I) N-heterocyclic carbene complex **i** was found to be efficient precatalyst for accessing bis(triazole) compound **1**, thus which was also utilized herein to prepare its analogue **2**.

Scheme 1 Synthesis of bis(triazoles) **1** and **2**

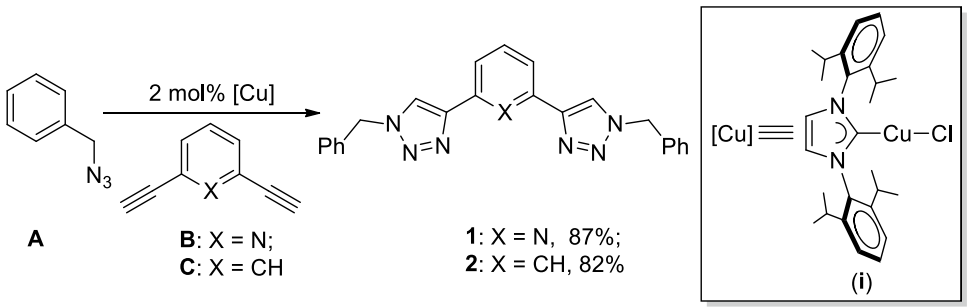

Synthesis of [NNN]-type pincer complexes bearing monodentate phosphines

First, pyridine-linked bis(triazole) **1** was treated with [Ru^{II}Cl$_2$(PPh$_3$)$_3$] in isopropanol successfully affording pincer complex *cis*-**3** in a moderate yield of 62% (Scheme 2).

In the ^{31}P NMR spectrum of *cis*-**3**, two doublets at 42.1 ppm and 37.7 ppm with a coupling constant of 30.4 Hz were observed, which is indicative of two *cis*-standing phosphine ligands. Such coordination mode can be further unambiguously confirmed by X-ray diffraction analysis (vide infra). Interestingly, previously reported Ru [NNN]-pincer/bis(phosphine) complexes [14–27] predominantly bear two mono-phosphines in *trans* positions. By contrast, the *cis*-configuration adopted by two phosphines in *cis*-**3** is much less common and unexpected,[7] since such coordination mode obviously increases the steric repulsion of the two bulky binding phosphines as indicated by the P–Ru–P angle amounting to 98.81(3)° (vide infra).

Complex *cis*-**3** shows moderate solubility in DMSO, isopropanol and CH_2Cl_2. Standing the solution of *cis*-**3** in d^6-DMSO at the ambient temperature for one week does not lead to the formation of any isomerized or decomposed products like *trans*-**3** (monitored by ^{31}P NMR), which demonstrates the high stability of such *cis*-oriented isomer.

Synthesis of [NCN]-type pincer complexes bearing monodentate phosphines

Then, following the procedure accessing *cis*-**3**, phenylene-based compound **2** was treated with [Ru^{II}Cl$_2$(PPh$_3$)$_3$]. NaOAc was added to assist the C-H activation and cyclometalation (Scheme 3). However, in this case, an inseparable mixture was always obtained despite several attempts. By evaporation of the solution of the crude product, we were able to obtain some single crystals which proved to be a Ru^{III} complex *trans*-**4**. The formation of *trans*-**4** clearly indicates that an oxidation of the metal center has occurred, which is likely due to the electron-rich feature of Ru^{II} center imparted by the strongly donating aryl anion-based NCN ligand. Notably, such instability is also in sharp contrast to the other known Ru^{II} [NCN] pincer analogues, which are reported to be fairly stable [25]. As expected, the two mono-phosphines are both perpendicular to the [NCN] coordination plane adopting a *trans*-orientation. The fact that all phosphines are *cis* to the aryl donor can be rationalized by the known *transphobia* effect.[8]

[7] To the best of our knowledge, there is only one report regarding Ru NNN pincer complexes bearing two *cis*-standing mono-phosphines. For this paper, see Ref. [15].

[8] For the report in which the term "*transphobia effect*" was coined, see [32].

Scheme 2 Synthesis of bis(phosphine) complex *cis*-**3**

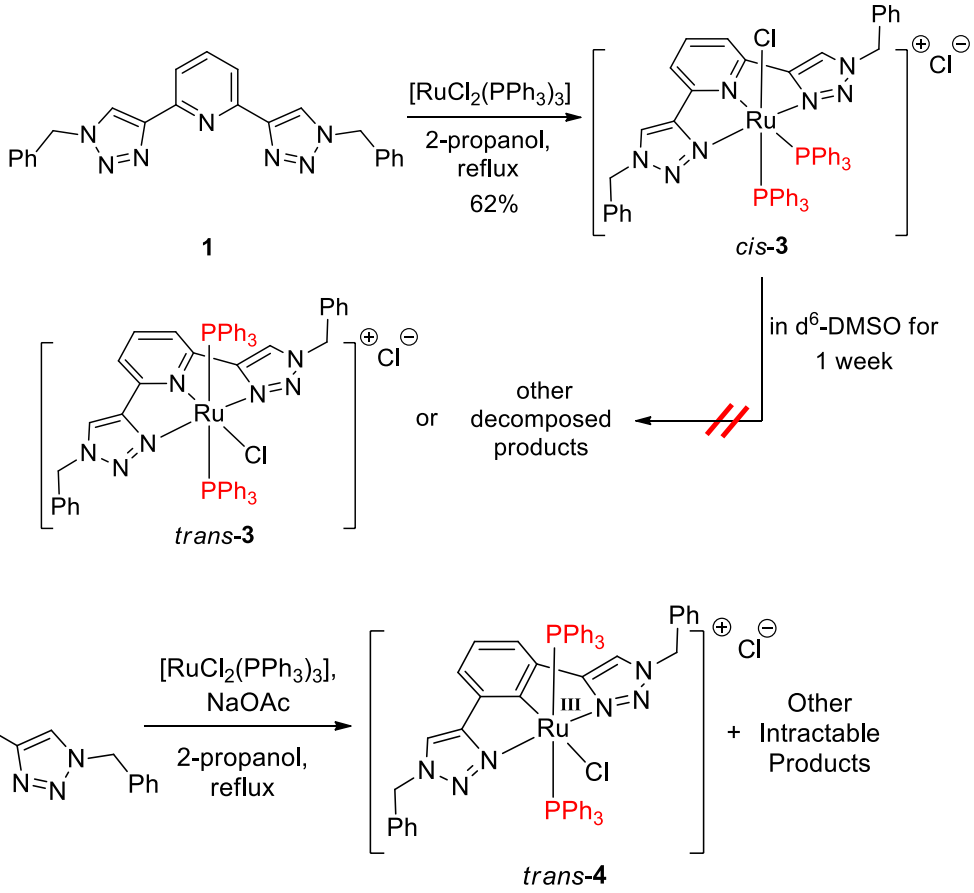

Scheme 3 Attempt to synthesize [NCN]-type pincer complex of ruthenium

Synthesis of pincer complexes bearing bidentate phosphines

In previous reports, Ru complexes bearing bidentate phosphines show superior catalytic performance in TH reactions compared to their counterparts with two monodentate phosphines [15]. Thus, to further modify the structure, two diphosphine ligands dppe and dppf were used, and via ligand exchange reactions, complexes **5** and **6** can be obtained in good yields (Scheme 4).

In the ^{1}H NMR spectra of **5**, the benzylic protons give two doublets at 5.37 ppm and 5.27 ppm with a coupling constant of ~ 15 Hz showing a "roofing effect". Such characteristics clearly indicate that the two NCH_2 hydrogen nuclei become diastereotopic thus resulting a geminal coupling. This is likely owing to the rigidity of the binding diphosphines making the N-C_{benzyl} bond rotation more difficult. ^{31}P NMR spectroscopic analyses provided additional evidence for their formations. In the case of **5**, two doublets at 65.8 and 59.3 ppm with a coupling constant of ~ 22 Hz were found, which can be assigned to the two *cis*-standing phosphorus donors in dppe ligand. Similar NMR features were also observed in the case of dppf analogue **6**. The formation of **5** was further verified by X-ray single-crystal diffraction study (vide infra).

Hydrido complexes

Previously, Ru–hydrido species have been proposed or proved to be key active intermediates in TH reactions.[9] The [NNN]-type pincer platform employed herein may make it more feasible to access certain stable enough Ru–H complexes. Thus, *cis*-**3** serving as a representative was treated with K_2CO_3, and ^{i}PrOH was used as the solvent as well as the hydrogen donor (Scheme 5).

^{1}H NMR spectroscopic analysis of the crude product revealed the formations of several Ru–H complexes. The selected region of the spectrum showing the hydrido signals is given in Fig. 2. The splitting pattern and coupling constant ($^{2}J_{P–Ru–H}$) proved to be diagnostic, which are used to assign and distinguish the as-formed major Ru–H species. It has been known that the coupling between P and H atoms *trans* to each other ($^{2}J_{P(trans)–M–H}$) is markedly greater than

[9] For a review, see [33].

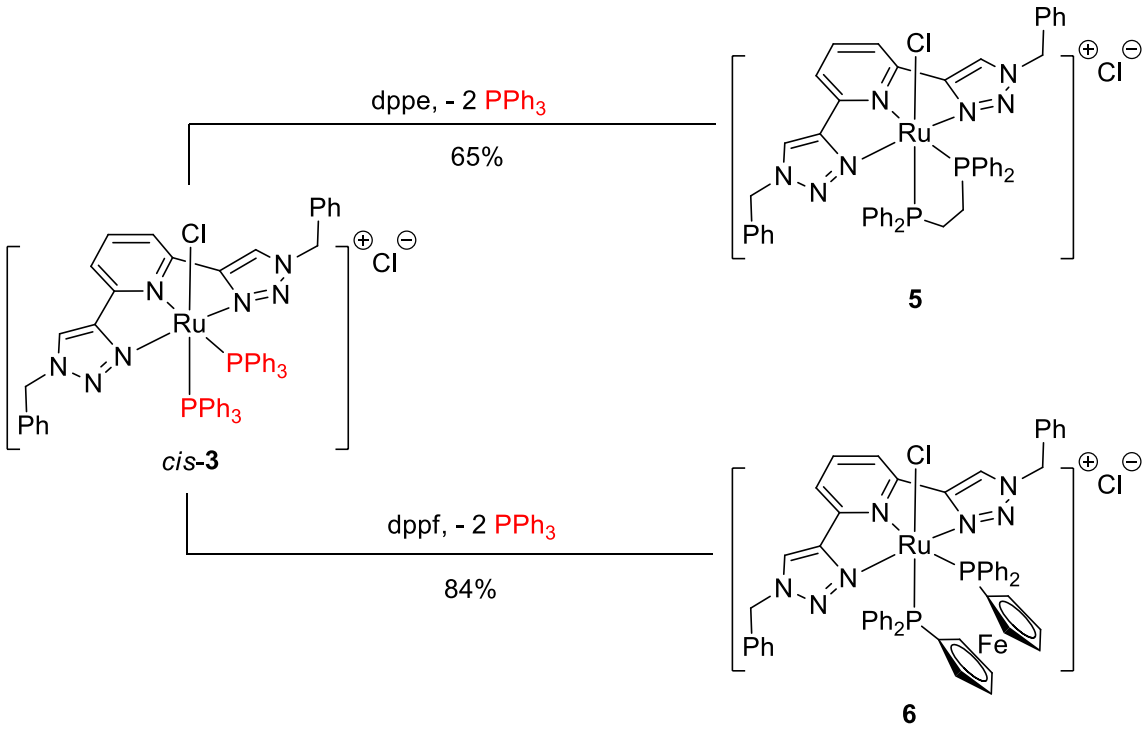

Scheme 4 Synthesis of diphosphine complexes **5** and **6**

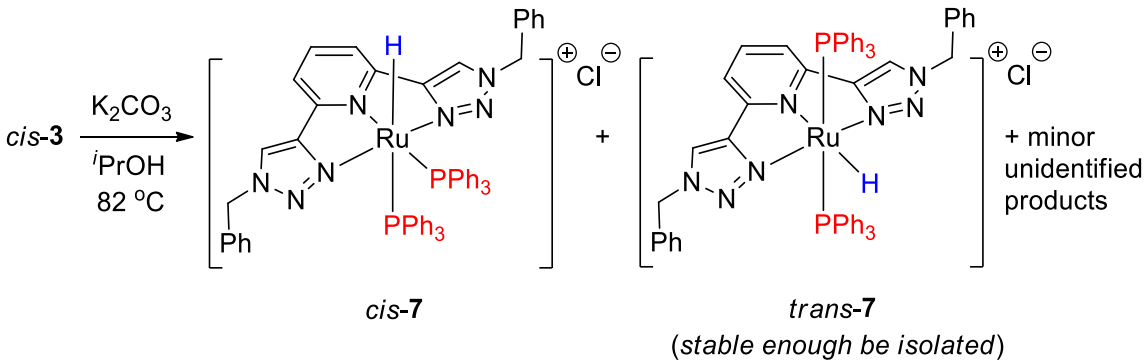

Scheme 5 Synthesis of ruthenium–hydrido complexes

that ($^2J_{P(cis)–M–H}$) involving two *cis*-standing nuclei [34]. The coupling constant in the former case is generally > 80 Hz, while the latter one is only less than 40 Hz. Thus, the species giving a triplet at − 7.48 ppm with a coupling constant of 24 Hz is assigned to *trans*-**7**. These ^{1}H NMR features are also in line with the previously reported analogues [35–38]. In addition, a doublet of doublet at − 8.64 ppm with two coupling constants of 100 and 32 Hz was observed, which is assigned to the hydrido ligand of *cis*-**7**. Such NMR characteristics have been also observed in a previously reported analogue [15]. Finally, the minor Ru–H species giving rise to a doublet at − 10.69 ppm cannot be unambiguously identified at the current stage. The two dominant hydrido species (*trans*-**7** and *cis*-**7**) give an integration ratio of 1:1.2, clearly indicating that the *cis*-orientation adopted by the monophosphines of *cis*-**3** has been partially changed during the reaction.

In addition, ESI mass spectrometry further verifies the formation of Ru–H species by the base peaks observed at *m*/*z* 1020, 510 and 500 corresponding to the monocationic fragments [**7**–Cl]$^+$ as well as dicationic species [**7**–Cl–H]$^{2+}$ and [**7**–Cl–H + CH_3CN]$^{2+}$.

By using column chromatography, *trans*-**7** can be isolated although in a low yield. By contrast, several attempts to isolate *cis*-**7** were to no avail, which may implicate a lower stability of such species versus *trans*-**7**. This is further

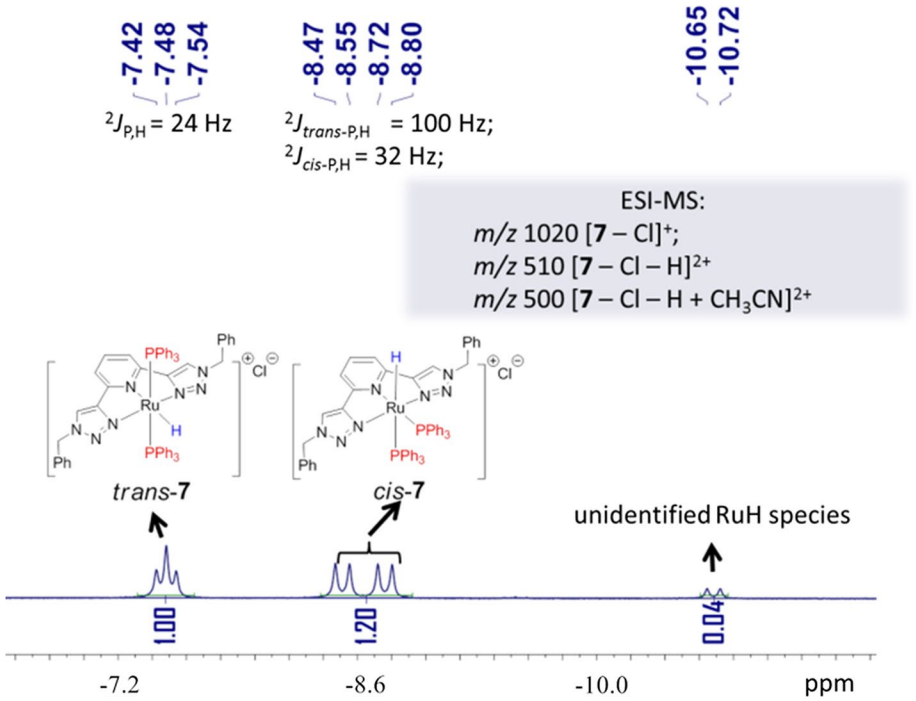

Fig. 2 Selected region of ^{1}H NMR spectrum of the crude product (including *trans*-**7** and *cis*-**7**, etc.) showing the hydrido signals

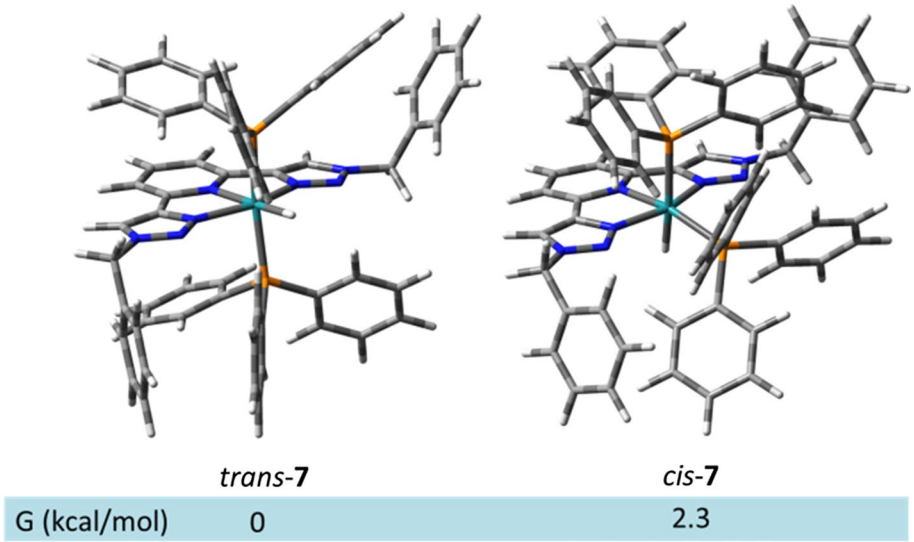

Fig. 3 DFT-optimized structures and calculated relative Gibbs free energies of *trans*-**7** and *cis*-**7**. DFT settings: M11-L/6-31G(d) (for C H N P); ECP-SDD (for Ru)

supported by DFT calculations, which indicates that the Gibbs free energy of *cis*-**7** (Fig. 3) is 2.3 kcal/mol higher compared to that for the *trans* isomer.

X-ray diffractions

The solid-state structures of complexes *cis*-**3**, *trans*-**4**, **5** are depicted in Fig. 4. Selected important crystallographic data are listed in Table SI-1 (ESI). All ruthenium complexes adopt distorted octahedral geometry. Notably, in the case of *cis*-**3**, the P1-Ru–P2 bond angle is found to be remarkably larger than 90°, which is owing to the severe repulsion of the two sterically demanding phosphines. Probably due to the same reason, the Ru-P bond distances of *cis*-**3** are significantly longer compared to those in the diphosphine counterpart **5**.

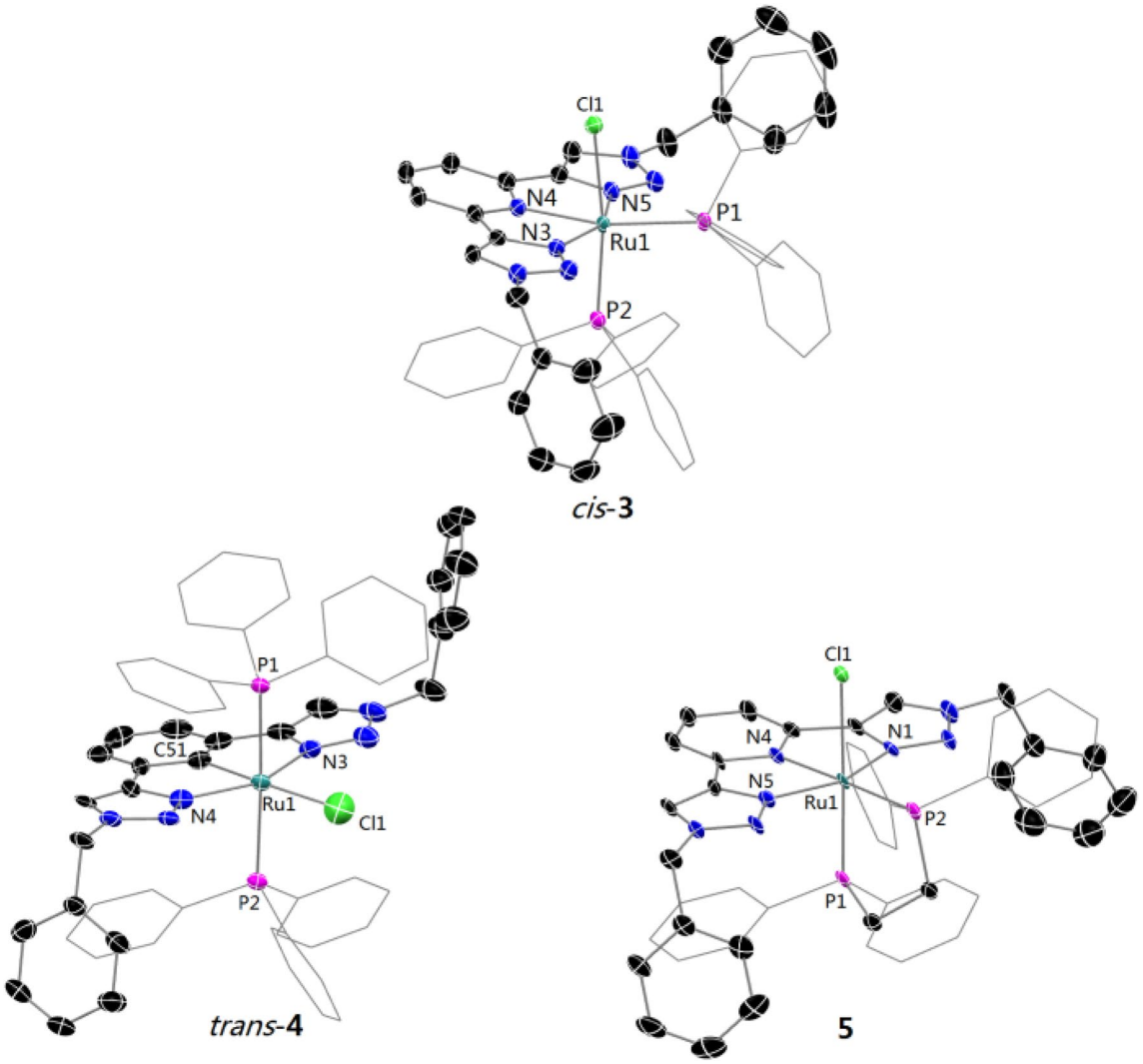

Fig. 4 Molecular structure of *cis*-**3**, *trans*-**4** and **5** showing 50% probability ellipsoids. Hydrogen atoms, solvent molecules and counter anions have been omitted for clarity. Selected bond lengths (Å) and bond angles (deg): for *cis*-**3**: P2-Ru1-P1 98.81(3), Ru1-Cl1 2.4531(7), Ru1-P1 2.3817(7), Ru1-P2 2.3128(8); for *trans*-**4**: P1-Ru1-P2 175.97(8), P1-Ru1 2.3852(19), P2-Ru1 2.399(2). For **5**: P1-Ru1-P2 83.96(4), Ru1-Cl1 2.4856(12), Ru1-P1 2.2684(13), Ru1-P2 2.3134(12)

Catalytic TH reactions

Ru-mediated transfer hydrogenation (TH) of ketones has evolved to become a powerful approach to access alcohols under mild conditions.[10] With all ruthenium pincer complexes in hand, their catalytic activities in TH reactions were then examined and compared. In the model reaction, acetophenone (**8**) was employed as the substrate, and 0.1 mol% of Ru complex was used as the catalyst (Table 1). Isopropanol was chosen to serve as the solvent as well as the hydrogen donor, since it is cheap and environmentally benign. In addition, such hydrogen donor and its dehydrogenated product (i.e., acetone) can be very easily removed from the catalytic system via simple evaporation.

Despite these exciting precedents, easily accessible, robust, efficient and chemoselective Ru-based catalytic systems are still strongly appealing. First, the reported [NNN]-pincer ligands used for THs typically require multiple and sophisticated synthetic steps, and in certain cases undesired harsh conditions are needed. In addition, the known Ru-mediated catalytic systems predominantly focus on the transformations of simple ketones, while THs of α,β-unsaturated ketones are much less investigated.[11]

The reaction in the absence of base gives no formation of the desired product (Entry 1). When K_2CO_3 was utilized as the base, a low yield was obtained at a reaction time of 2 h. A further extension of the reaction time to 24 h leads to

[10] For selected reviews on TH reactions, see [39–43].

[11] For a review on Ru-mediated THs of enones, see [44–48].

Table 1 Catalytic transfer hydrogenations between ketones and isopropanol

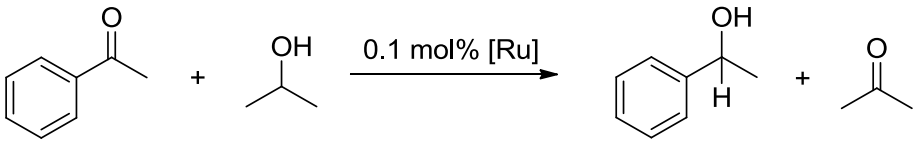

8 **9**

Entry	Cat.	Base	*t* (h)	Yield[a] (%)
1	*cis*-**3**	–	2	0
2	*cis*-**3**	K_2CO_3	2	9
3	*cis*-**3**	K_2CO_3	24	82
4	*cis*-**3**	^{i}PrOK	0.5	62
5	*cis*-**3**	^{i}PrOK	2	98
6	**5**	^{i}PrOK	2	6
7	**6**	^{i}PrOK	2	10
8	*trans*-**7**	^{i}PrOK	2	45

Condition: 2 mmol of ketone, 2 mL of isopropanol, 2 mol% of base, 0.1 mol% of Ru catalyst, 82 °C

[a]Yields were determined using ^{1}H NMR spectroscopy

a largely improved yield (Entry 2 vs. Entry 3). A stronger base ^{i}PrOK proved to be much superior. A moderate conversion can be achieved at only 30 min, and the reaction can proceed near quantitatively in 2 h (Entry 5). By contrast, diphosphine complexes **5** and **6** exhibited much poorer performance (Entries 6/7 vs. Entry 5). Such observation is in sharp contrast to some previous reports, in which pincer-type precatalysts coligated with diphosphines show comparable or even superior catalytic behaviors compared to their mono-phosphine counterparts [15]. Interestingly, when Ru–H complex *trans*-**7** was utilized as the catalyst under the same condition, a much lower yield was obtained (entry 7 vs. entry 5). This dramatic difference may imply that *trans*-**7** is not the primary Ru–H intermediate during the catalysis of *cis*-**3**, and less stable Ru–H species *cis*-**7** is likely to be a more significant catalytic contributor.

The best performer complex *cis*-**3** was chosen as the catalyst to further expand the substrate scope (Table 2). For most of the sterically and electronically varied simple ketones, good yields can be obtained (entries 1–3). No activity was observed for the case of stilbene indicating the catalytic inertness toward simple carbon–carbon double bond (entry 4). In addition, α,β-unsaturated ketones were also used as the substrates to test the catalytic chemoselectivity. Enones are known to be less active in TH reactions, and thus, the catalyst loading was improved to 1 mol%. Benzylideneacetone (**18**) is one of the most studied enones for TH catalysis. Interestingly, when this substrate was employed, the TH reaction proceeded in a high chemoselective manner giving a moderate yield (entry 5). Only the C=C double bond was reduced, and no alcohol-containing products **19b** and **19c** were observed. Such behavior is different with most of the reported Ru-based catalysts [44–48], and to the best of our knowledge, only very few Ru complexes exhibit similar performance for this particular substrate [26, 46]. Such chemoselectivity is found to be sensitive to the substrate variation. When phenyl-substituted enone **20** was utilized, completely hydrogenated species **21c** was found to be the predominant product. The attachment of a chlorine substituent to benzylideneacetone also brings a decreased selectivity and activity (entry 7). The reason of such enone-dependent chemoselectivity is not clear at the current stage and remains to be further explored in the future.

Conclusion

In conclusion, we have reported a conveniently constructed Ru pincer system supported by a triazole-based tridentate ligand platform and coligated with phosphines. In the case employing phenylene-bridged [NCN]-pincer ligand, an oxidation of Ru^{II} to Ru^{III} was observed. In contrast, robust pincer complexes can be accessed when pyridine-linked bis(triazoles) was used as the supporting ligand. For Ru–chlorido complex **3**, the two mono-phosphines are found to bind in an unusual *cis*-standing fashion, which is different from most of the precedents. Such binding mode is (partially) altered during the conversion of **3** to Ru–H complex **7**. Experimental and computational studies implicate that *trans*-oriented Ru–H species is more stable compared to the

Table 2 Transfer hydrogenations of ketones and enones in isopropanol

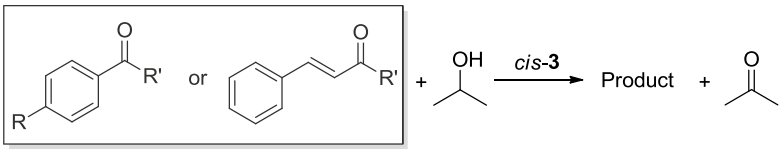

Ent	Ketone/enone	*t*	Product and yield (%) [a]
1	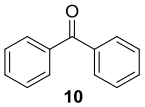 **10**	2	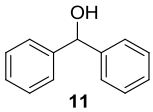 **11** (81%)
2	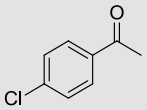 **12**	2	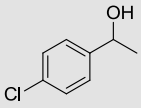 **13** (79%)
3	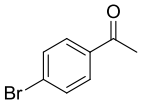 **14**	2	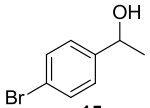 **15** (43%)
4	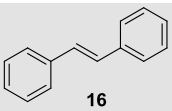 **16**	24	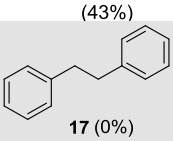 **17** (0%)
5	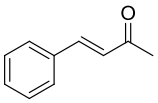 **18**	24	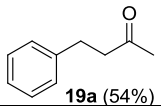 **19a** (54%) 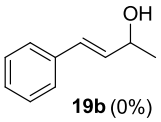 **19b** (0%) 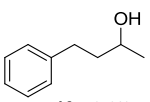 **19c** (0%)
6	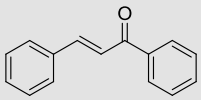 **20**	24	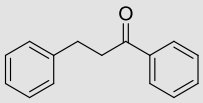 **21a** (8%) 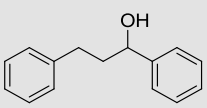 **21c** (65%) 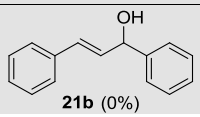 **21b** (0%)
7	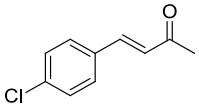 **22**	24	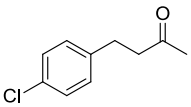 **23a** (15%) 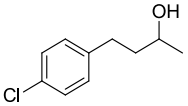 **23c** (14%) 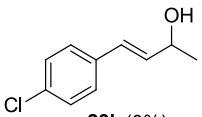 **23b** (0%)

Table 2 (continued) Condition: 2 mmol of the substrate, 2 mL of isopropanol, 2 mol% of base, 0.1 mol% (for entries 1–3) and 1 mol% (for entries 4–7) of Ru catalyst, 82 °C

[a]Yields were determined using ^{1}H NMR spectroscopy using 1,3,5-trimethoxybenzene as the internal standard

cis-isomer. In addition, diphosphine complexes **5/6** can be prepared via ligand exchanges of *cis*-**3**. Catalytic studies on TH reactions indicate: (1) mono-phosphine complex *cis*-**3** shows much superior performance compared to diphosphine counterparts **5/6**; (2) the current catalytic system is likely to be [Ru–H]-mediated, but *trans*-**7** may not be the main catalytic contributor; (3) the best performer *cis*-**3** exhibits good activity for most of simple ketones and shows high chemoselectivity in the case of benzylideneacetone as the enone substrate. Additionally, the selectivity is found to be highly dependent on the enone skeletons.

The "popular" btp pincer platform (btp = bis(1,2,3-triazol-4-yl)-pyridine), although extensively studied, is applied for Ru-based catalysis for the first time. The structural elucidations and catalytic investigations of Ru–btp system studied herein will facilitate the search for further applications of such complexes. In addition, the uncommon phosphine binding modes and high chemoselectivity in TH of enones (although limited to certain cases) have implications for the design of corresponding systems. A more detailed mechanistic study in catalysis as well as further structure variations of Ru pincer complexes is underway in our laboratory.

Experimental section

General considerations

If not mentioned otherwise, all reagents and solvents were used as received without further purification. ^{1}H, ^{13}C and ^{31}P NMR spectra were recorded on a 600 MHz or 400 MHz spectrometer. The chemical shifts (δ) were internally referenced to the residual solvent signals based on literature [49]. ESI mass spectra were measured using an Agilent 6540 Q-TOF mass spectrometer. X-ray single-crystal diffractions were done using a Rigaku XtaLAB P200 MM003 diffractometer. Elemental analyses were done on a vario EL cube elemental analyzer.

General procedure for the synthesis of 1 and 2

A round-bottom flask (50 mL) was charged with benzyl azide (2.5 mmol), 2,6-diethynylbenzene (or 1,3-diethynylbenzene, 1 mmol) and the precatalyst [IPrCuCl] (9.8 mg, 0.02 mmol). A mixture of ethanol (15 mL) and deionized water (5 mL) was added. The reaction mixture was stirred for 24 h at 60 °C. All the volatiles were removed *in vacuo*. The residue was washed with ether (3 × 5 mL), and the solid pumped dry in *vacuo* affording the product as an off-white solid (87% for **1** and 82% for **2**). The ^{1}H NMR spectroscopic data agree with the reported [28–30].

Synthesis of *cis*-3

Compound **2** (78.7 mg, 0.2 mmol), $[RuCl_2(PPh_3)_3]$ (191.8 mg, 0.2 mmol) and isopropanol (5 mL) were mixed in a Schlenk tube under N_2. The tube was sealed, and the reaction mixture was stirred for 3 h at 85 °C. After cooling down to the ambient temperature, the resulting precipitate was collected and washed with ethyl acetate (3 × 5 mL) followed by diethyl ether (3 × 5 mL). All the volatiles were removed in *vacuo* affording the product as a yellow solid (135 mg, 62%). ^{1}H NMR (600 MHz, d_6-DMSO): δ (ppm) 8.99 (s, 2H, Triazole-C^5–H), 8.04 (t, 1H, Ar–H, $^{3}J_{H,H}$ = 7.8 Hz), 7.86 (d, 2H, Ar–H, $^{3}J_{H,H}$ = 7.8 Hz), 7.43–7.14 (m, 30H, Ar–H), 6.73 (br s, 5H, Ar–H), 6.33 (br s, 5H, Ar–H), 5.60 (s, 4H, NCH_2). ^{13}C NMR (150 MHz, d_6-DMSO): δ (ppm) 149.9, 148.8, 138.2, 135.5, 135.2, 134.5 (d, $J_{C,P}$ = 9.6 Hz), 134.4, 132.6, 130.9, 130.6, 129.6, 129.1, 128.9, 128.8, 128.2, 127.5 (d, $J_{C,P}$ = 9 Hz), 127.1 (d, $J_{C,P}$ = 9.2 Hz), 125.3, 119.6 (Ar–C), 55.0 (NCH_2). ^{31}P NMR (162 MHz, d_6-DMSO): δ (ppm) 42.1 (d, $^{2}J_{P,P}$ = 30.4 Hz), 37.7 (d, $^{2}J_{P,P}$ = 30.4 Hz). MS (ESI): *m/z* 1054 $[M–Cl]^+$. Anal. Calcd. for $C_{59}H_{49}Cl_2N_7P_2Ru$: C, 65.01; H, 4.53; N, 9.00; Found: C, 65.40; H, 4.35; N, 9.19%.

Synthesis of 5

Complex **3** (87.2 mg, 0.08 mmol), 1,2-bis(diphenylphosphino)ethane (31.9 mg, 0.08 mmol) and isopropanol (4 mL) were mixed in a Schlenk tube. The tube was sealed, and the reaction mixture was stirred at 82 °C overnight. After cooling down to the ambient temperature, all the volatiles were removed *in vacuo*. The residue was washed with diethyl ether (3 × 5 mL) and purified using flash column chromatography (SiO_2, CH_2Cl_2:CH_3OH (v:v) = 8:1) affording the product as a yellow solid (50 mg, 65%). ^{1}H NMR (600 MHz, d_6-DMSO): δ (ppm) 8.93 (s, 2H, Triazole-C^5–H), 8.23 (t, 1H, Ar–H, $^{3}J_{H,H}$ = 7.8 Hz), 8.13–8.09 (m, 6H, Ar–H), 7.45–7.42 (m, 7H, Ar–H), 7.35–7.33 (m, 4H, Ar–H), 7.18–7.16 (m, 6H, Ar–H), 6.87–6.84 (m, 4H, Ar–H), 6.56–6.53 (m, 4H, Ar–H), 5.37 (d, 2H, NCH_2, $^{3}J_{H,H}$ = 14.6 Hz), 5.27 (d, 2H, NCH_2, $^{3}J_{H,H}$ = 14.6 Hz), 2.98–2.90 (m, 2H, CH_2), 2.64–2.56 (m, 2H, CH_2). ^{13}C NMR (150 MHz, d_6-DMSO): δ (ppm) 149.5, 148.5, 138.6, 136.4, 136.1, 134.2, 132.8 (d, $J_{C,P}$ = 9.9 Hz), 131.1, 130.9, 129.9 (d, $J_{H,P}$ = 9.0 Hz), 129.7, 129.5, 128.9, 128.8, 128.6, 128.1 (d,

$J_{C,P}$ = 9.2 Hz), 127.7 (d, $J_{C,P}$ = 9.5 Hz), 125.2, 119.6 (Ar–C), 54.5 (NCH_2), the resonances of CH_2 (dppe) overlap with the signal of DMSO. ^{31}P NMR (162 MHz, d_6-DMSO): δ (ppm) 65.8 (d, $^2J_{P,P}$ = 22.2 Hz), 59.3 (d, $^2J_{P,P}$ = 22.2 Hz). MS (ESI): *m/z* 928 $[M–Cl]^+$. Anal. Calcd. for $C_{49}H_{43}Cl_2N_7P_2Ru$: C, 61.06; H, 4.50; N, 10.17; Found: C, 60.80; H, 4.75; N, 9.86%.

Synthesis of 6

Complex **3** (87.2 mg, 0.08 mmol), dppf (44.4 mg, 0.08 mmol) and isopropanol (4 mL) were mixed in a Schlenk tube. The tube was sealed, and the reaction mixture was stirred for 5 d at 82 °C. After cooling down to the ambient temperature, all the volatiles were removed *in vacuo*. The crude product was washed with diethyl ether (3 × 5 mL) and dried *in vacuo* affording the product as a yellow solid (75.3 mg, 84%). ^{1}H NMR (600 MHz, d_6-DMSO): δ (ppm) 9.06 (s, 2H, Triazole-C^5–H), 8.01–7.97 (m, 5H, Ar–H), 7.84–7.82 (m, 2H, Ar–H), 7.52–7.40 (m, 12H, Ar–H), 7.33–7.30 (m, 4H, Ar–H), 7.18–7.15 (m, 2H, Ar–H), 6.76–6.72 (m, 4H, Ar–H), 6.52–6.47 (m, 4H, Ar–H), 5.70 (d, 2H, NCH_2, $^2J_{H,H}$ = 21.6 Hz), 5.52 (d, 2H, NCH_2, $^2J_{H,H}$ = 21.6 Hz). 4.41–4.34 (m, 6H, Ar–H). 4.18 (br s, 2H, Ar–H). ^{13}C NMR (150 MHz, d_6-DMSO): δ (ppm) 150.0 (d, $J_{C,P}$ = 2.1 Hz), 148.5, 138.2, 137.9, 137.7, 134.8 (d, $J_{C,P}$ = 10.1 Hz), 134.3, 132.2, 132.1, 131.9, 129.6, 129.1, 129.0 (d, $J_{C,P}$ = 3.9 Hz), 128.9, 127.2 (d, $J_{C,P}$ = 9.2 Hz), 126.9 (d, $J_{C,P}$ = 9.2 Hz), 125.4, 119.5, 80.4 (dd, $J_{C,P}$ = 3.6, 43.4 Hz), 77.6 (dd, $J_{C,P}$ = 2.8, 52.1 Hz), 74.6 (dd, $J_{C,P}$ = 9.3, 13.1 Hz), 73.2 (d, $J_{C,P}$ = 4.7 Hz), 71.5 (d, $J_{C,P}$ = 4.7 Hz), 62.8 (Ar–C), 55.1 (NCH_2). ^{31}P NMR (133 MHz, d_6-DMSO): δ (ppm) 43.5 (d, $^2J_{P,P}$ = 26.6 Hz), 35.1 (d, $^2J_{P,P}$ = 26.6 Hz). MS (ESI): *m/z* 1084 $[M–Cl]^+$. Anal. Calcd. for $C_{57}H_{47}Cl_2FeN_7P_2Ru$: C, 61.14; H, 4.23; N, 8.76; Found: C, 61.50; H, 4.11; N, 8.38%.

Synthesis of *trans*-7

Under a nitrogen atmosphere, complex **3** (109 mg, 0.1 mmol), K_2CO_3 (138.2 mg, 1 mmol) and isopropanol (5 mL) were mixed in a Schlenk tube. The tube was sealed, and the reaction mixture was stirred for 8 h at 82 °C. After cooling down to the ambient temperature, all the volatiles were removed *in vacuo*. Dichloromethane was added, and the insoluble was filtered off. The organic phase was collected and dried. The crude product was purified using column chromatography (SiO_2, CH_2Cl_2:CH_3OH (v:v) = 8:1) affording the product as a yellow solid (12 mg, 11%). ^{1}H NMR (600 MHz, d_6-DMSO): δ (ppm) 8.49 (s, 2H, Triazole-C^5–H), 7.63–7.55 (m, 4H, Ar–H), 7.43–7.08 (m, 36H, Ar–H), 6.90–6.89 (m, 3H, Ar–H), 5.29 (s, 4H, NCH_2),-7.49 (t, 1H, $^2J_{H,P}$ = 24 Hz). ^{13}C NMR (150 MHz, d_6-DMSO): δ (ppm) 149.1, 146.4, 134.7, 133.3, 133.2, 133.0, 132.8, 132.7, 132.6, 132.54, 132.50, 132.0 (d, $J_{C,P}$ = 2.6 Hz), 131.5 (d, $J_{C,P}$ = 9.6 Hz), 129.0, 128.9, 128.8, 128.75, 128.72, 128.4, 128.0, 127.62, 127.59, 127.56, 123.4, 117.9 (Ar–C), 54.2 (NCH_2). ^{31}P NMR (162 MHz, d_6-DMSO): δ (ppm) 49.3 (s). Anal. Calcd. for $C_{59}H_{50}ClN_7P_2Ru$: C, 67.13; H, 4.77; N, 9.29; Found: C, 67.42; H, 4.57; N, 9.46%.

Catalytic transfer hydrogenations

In a typical run, to a 25-mL Schlenk tube, the substrate, Ru catalyst and 2-propanol (2 mL) were added under a nitrogen atmosphere. The tube was sealed, and the reaction mixture was heated and stirred at 82 °C for 10 min. After addition of the base, the reaction mixture was stirred and heated for in a reaction time indicated in Table 1 or Table 2. After cooling down to the ambient temperature, all the volatiles were removed *in vacuo*. The crude product was analyzed by ^{1}H NMR spectroscopy.

X-ray diffraction studies

Structural solution was carried out with the Olex2 program [50]. The structure was solved using direct methods. All non-hydrogen atoms were generally given anisotropic displacement parameters in the final model. All H atoms were put at calculated positions.

Refinement model description for *cis*-**3**: (1) fixed Uiso at 1.2 times of all C(H) groups and all C(H,H) groups; fixed Uiso at 1.5 times of all O(H,H) groups; (2) restrained distances.

O1–H1C=O1–H1D, 0.84 with sigma of 0.01; H1C-H1D, 1.39 with sigma of 0.02; H1A–H1C, −2.1 with sigma of 0.02; (3) secondary CH_2 refined with riding coordinates: C1(H1A,H1B), C17(H17A,H17B), C24(H24A,H24B), C25(H25A,H25B); aromatic/amide H refined with riding coordinates: C3–C8, C11–13, C16, C19(H19), C20(H20), C21(H21), C22(H22), C23(H23), C27(H27), C28(H28), C29(H29), C30(H30), C31(H31), C33(H33), C34(H34), C35(H35), C36(H36), C37(H37), C39(H39), C40(H40), C41(H41), C42(H42), C43(H43), C45(H45), C46(H46), C47(H47), C48(H48), C49(H49), C50(H50), C51(H51), C52(H52), C53(H53), C54(H54), C57(H57), C58(H58), C59(H59), C60(H60), C61(H61).

Refinement model description for *trans*-**4**: (1) twinned data refinement scales: 0.674(13), 0.326(13); (2) fixed Uiso at 1.2 times of all C(H) groups and all C(H,H) groups; (3) Uiso/Uaniso restraints and constraints: Uanis(Ru1) ≈ Ueq with sigma of 0.01 and sigma for terminal atoms of 0.02; (4) others: fixed Sof: Cl1(0.5) Cl1′(0.5) (5) secondary CH_2 refined with riding coordinates: C43(H43A,H43B),

C54(H54A,H54B), C61(H61A,H61B); aromatic/amide H refined with riding coordinates: C2(H2), C3(H3), C4(H4), C5(H5), C6(H6), C8(H8), C9(H9), C10(H10), C11(H11), C12(H12), C14(H14), C15(H15), C16(H16), C17(H17), C18(H18), C20(H20), C21(H21), C22(H22), C23(H23), C24(H24), C26(H26), C27(H27), C28(H28), C29(H29), C30(H30), C32(H32), C33(H33), C34(H34), C35(H35), C36(H36), C37(H37), C38(H38), C39(H39), C40(H40), C41(H41), C44(H44), C47(H47), C48(H48), C49(H49), C53(H53), C56(H56), C57(H57), C58(H58), C59(H59), C60(H60).

Refinement model description for **5**: (1) fixed Uiso at 1.2 times of all C(H) groups and all C(H,H) groups; at 1.5 times of all C(H,H,H) groups and all O(H) groups; (2) Uiso/Uaniso restraints and constraints: Uanis(N2) ≈ Ueq, Uanis(N7) ≈ Ueq with sigma of 0.005 and sigma for terminal atoms of 0.01; Uanis(N3) ≈ Ueq, Uanis(O3) ≈ Ueq: with sigma of 0.005 and sigma for terminal atoms of 0.01; Uanis(C24) ≈ Ueq, Uanis(C7) ≈ Ueq: with sigma of 0.005 and sigma for terminal atoms of 0.01; (3) rigid body (RIGU) restrains all non-hydrogen atoms with sigma for 1–2 distances of 0.004 and sigma for 1–3 distances of 0.004; (4) ternary CH refined with riding coordinates: C41(H41), C53(H53), C57(H57); secondary CH_2 refined with riding coordinates: C13(H13A,H13B), C14(H14A,H14B), C27(H27A,H27B), C46(H46A,H46B); aromatic/amide H refined with riding coordinates: C2(H2), C3(H3), C4(H4), C5(H5), C6(H6), C8(H8), C9(H9), C10(H10), C11(H11), C12(H12), C16(H16), C17(H17), C18(H18), C19(H19), C20(H20), C22(H22), C23(H23), C24(H24), C25(H25), C26(H26), C28(H28), C29(H29), C30(H30), C31(H31), C32(H32), C34(H34), C37(H37), C38(H38), C39(H39), C45(H45), C48(H48), C49(H49), C50(H50), C51(H51), C52(H52); idealized Me refined as rotating group: C60(H60A,H60B,H60C), C61(H61A,H61B,H61C), C40(H40A,H40B,H40C), C42(H42A,H42B, H42C), C54(H54A,H54B,H54C), C55(H55A,H55B,H55C), C56(H56A,H56B,H56C), C58(H58A, H58B,H58C); idealized tetrahedral OH refined as rotating group: O1(H1), O3(H3A), O4(H4A).

A summary of the most important crystallographic data is given in Table SI-1. CCDC 1922403-1922405 contain the supplementary crystallographic data for this paper. These data can be obtained free of charge from the Cambridge Crystallographic Data Centre via www.ccdc.cam.ac.uk/data_request/cif.

Acknowledgements The authors thank "General Project of Scientific Research Program of Beijing Education Commission" (Grant No. KM201810028007), National Natural Science Foundation of China (Grant No. 21502122) and Beijing Natural Science Foundation (Grant No. 2192012) for financial support. The author Dr. Shuai Guo also highly appreciates the support from Yenching Young Scholar Cultivation Program of Capital Normal University.

Compliance with ethical standards

Conflict of interest The authors declare that they have no conflict of interest.

References

1. Byrne JP, Kitchen JA, Gunnlaugsson T (2014) Chem Soc Rev 43:5302
2. Haldón E, Nicasio MC, Pérez PJ (2015) Org Biomol Chem 13:9528
3. Liang L, Astruc D (2011) Coord Chem Rev 255:2933
4. Hein JE, Fokin VV (2010) Chem Soc Rev 39:1302
5. Meldal M, Tornøe CW (2008) Chem Rev 108:2952
6. Kolb HC, Finn MG, Sharpless KB (2004) Angew Chem Int Ed 2001:40
7. Schulze B, Friebe C, Hager MD, Winter A, Hoogenboom R, Görls H, Schubert US (2009) Dalton Trans 5:787
8. Yang W, Zhong Y (2013) Chin J Chem 31:329
9. Byrne JP, Kitchen JA, Kotova O, Leigh V, Bell AP, Boland JJ, Albrecht M, Gunnlaugsson T (2014) Dalton Trans 43:196
10. Gunanathan C, Milstein D (2014) Chem Rev 114:12024
11. Younus HA, Su W, Ahmad N, Chen S, Verpoort F (2015) Adv Synth Catal 357:283
12. Younus HA, Ahmad N, Su W, Verpoort F (2014) Coord Chem Rev 276:112
13. Freeman GR, Williams JAG (2013) Top Organomet Chem 40:89
14. Deng H, Yu Z, Dong J, Wu S (2005) Organometallics 24:4110
15. Wang L, Liu T (2018) Chin J Catal 39:327
16. Wang Q, Chai H, Yu Z (2017) Organometallics 36:3638
17. Chai H, Liu T, Yu Z (2017) Organometallics 36:4136
18. Chai H, Wang Q, Liu T, Yu Z (2016) Dalton Trans 45:17843
19. Wang Q, Wu K, Yu Z (2016) Organometallics 35:1251
20. Chai H, Liu T, Wang Q, Yu Z (2015) Organometallics 34:5278
21. Menéndez-Pedregal E, Vaquero M, Lastra E, Gamasa P, Pizzano A (2015) Chem Eur J 21:549
22. Li K, Niu J-L, Yang M-Z, Li Z, Wu L-Y, Hao X-Q, Song M-P (2015) Organometallics 34:1170
23. Paul B, Chakrabarti K, Kundu S (2016) Dalton Trans 45:11162
24. Shi J, Hu B, Chen X, Shang S, Deng D, Sun Y, Shi W, Yang X, Chen D (2017) ACS Omega 2:3406
25. Toda T, Saitoh K, Yoshinari A, Ikariya T, Kuwata S (2017) Organometallics 36:1188
26. Melle P, Manoharan Y, Albrecht M (2018) Inorg Chem 57:11761
27. Shi J, Hu B, Gong D, Shang S, Hou G, Chen D (2016) Dalton Trans 45:4828
28. Karthikeyan T, Sankararaman S (2009) Tetrahedron Lett 50:5834
29. Fabbrizzi P, Cicchi S, Brandi A, Sperotto E, van Koten G (2009) Eur J Org Chem 31:5423
30. Crowley JD, Bandeen PH, Hanton LR (2010) Polyhedron 29:70
31. Wang H, Zhang B, Yan X, Guo S (2018) Dalton Trans 47:528
32. Vicente J, Arcas A, Bautista D, Jones PG (1997) Organometallics 16:2127
33. Clapham SE, Hadzovic A, Morris RH (2004) Coord Chem Rev 248:2201
34. Bampos N, Field LD, Messerle BA (1993) Organometallics 12:2529
35. Wang Q, Chai H, Yu Z (2018) Organometallics 37:584
36. Du W, Wu P, Wang Q, Yu Z (2013) Organometallics 32:3083
37. Du W, Wang L, Wu P, Yu Z (2012) Chem Eur J 18:11550
38. Ye W, Zhao M, Du W, Jiang Q, Wu K, Wu P, Yu Z (2011) Chem Eur J 17:4737
39. Wang D, Astruc D (2015) Chem Rev 115:6621

40. Bartoszewicz A, Ahlsten N, Martín-Matute B (2013) Chem Eur J 19:7274
41. Li Y-Y, Yu S-L, Shen W-Y, Gao J-X (2015) Acc Chem Res 48:2587
42. Alonso F, Riente P, Yus M (2011) Acc Chem Res 44:379
43. Morris RH (2009) Chem Soc Rev 38:2282
44. Farrar-Tobar RA, Tin S, de Vries JG (2018) Organometallics for Green Catalysis. Topics Organomet Chem 63:193
45. Farrar-Tobar RA, Wei Z, Jiao H, Hinze S, de Vries JG (2018) Chem Eur J 24:2725
46. Melle P, Albrecht M (2019) Chimia 73:299
47. Horn S, Gandolfi C, Albrecht M (2011) Eur J Inorg Chem 18:2863
48. Liu T, Chai H, Wang L, Yu Z (2017) Organometallics 36:2914
49. Fulmer GR, Miller AJM, Sherden NH, Gottlieb HE, Nudelman A, Stoltz BM, Bercaw JE, Goldberg KI (2010) Organometallics 29:2176
50. Dolomanov OV, Bourhis LJ, Gildea RJ, Howard JAK, Puschmann H (2009) J Appl Cryst 42:339